

Validation of SAG-dependent Cerebellar Neurospheres (S-cNS) as a GCP culture

In a recent study from **Dr. Giuseppe Gianni-ni's lab** at the **Department of Molecular Medicine, University La Sapienza**, an innovative method to grow postnatal cerebellar **granule cell progenitors (GCPs)** as long term neurospheres was validated. The GCPs, stimulated by SAG (Smoothed Agonist) administration, undergo extensive self-renewal maintaining an active SHh pathway, or differentiate into GCs under appropriate conditions.

So far, scant and inefficient cellular models have been available to study GCPs in vitro. Explants from mice cerebella at 5-7 post-natal days (P5-7) are commonly used to establish SHh-stimulated short-term GCP cultures or long term neurospheres grown in "stem cell medium" containing a EGF/bFGF cocktail (GF). However, bFGF suppresses SHh activity, suggesting that these conditions are not appropriate to propagate cells with active SHh signaling.

In this study, the authors extensively characterized their **SAG-dependent cerebellar neurospheres (S-cNS)** in comparison to **GF-dependent cerebellar neurospheres (GF-cNS)**. They revealed that S-cNS, but not GF-cNS, presented a sustained functional activation of the SHh pathway similar to short-term GCP cultures. Moreover, cells in S-cNS were capable of EdU incorporation upon SAG treatment. Furthermore, the authors observed interesting differences in the overall expression profile between the two lines, thereby suggesting major disparities in the identity of the two populations of cerebellar neurospheres. In particular, S-cNS expressed higher levels of GCP markers such as ATOH1, PAX6 and Doublecortin (DCX) proteins (**Figure A**), the last showing a diffused expression in most cells comprising a neurosphere, while GF-cNS showed a significantly higher expression of the intermediate filament Nestin (**Figure B**), representative marker of neural stem cells (for further details see *Petroni et al., 2019*).

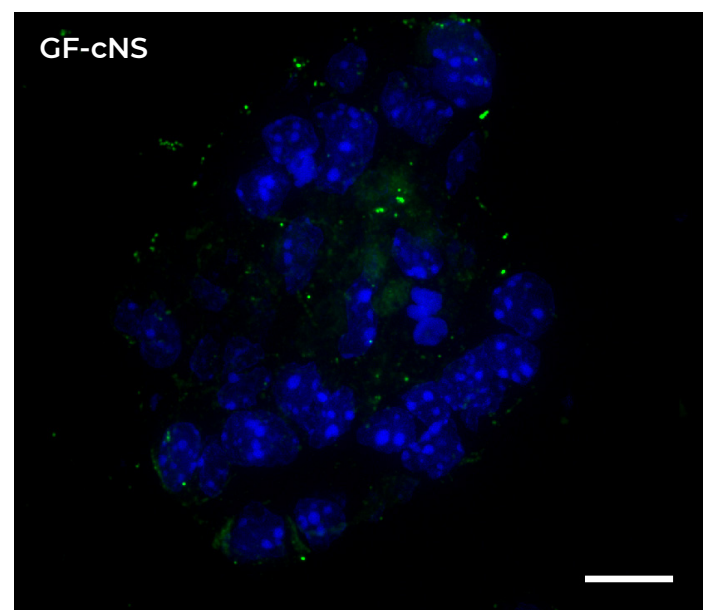
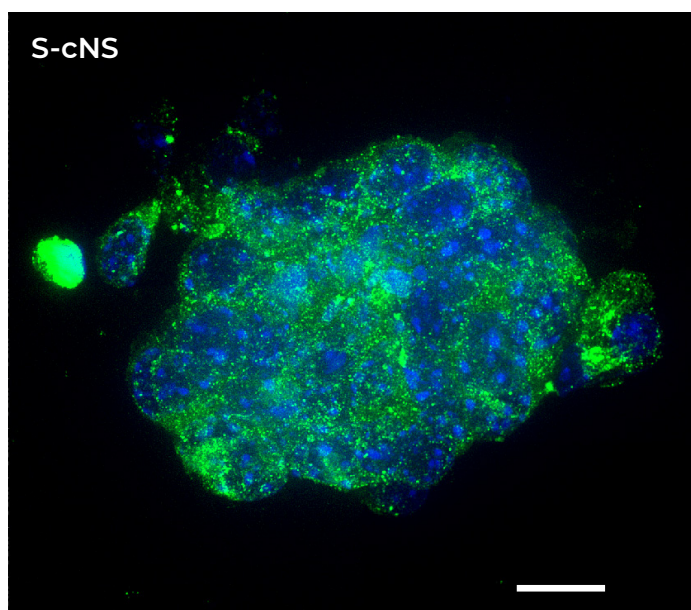


Figure A. Immunofluorescence analysis of DCX protein.

S-cNS and GF-cNS neurospheres stained for DCX (green) and DNA (blue). S-cNS neurospheres, unlike GF-cNS, show a diffused DCX localization in most cells. Scale bar, 10 μ m.

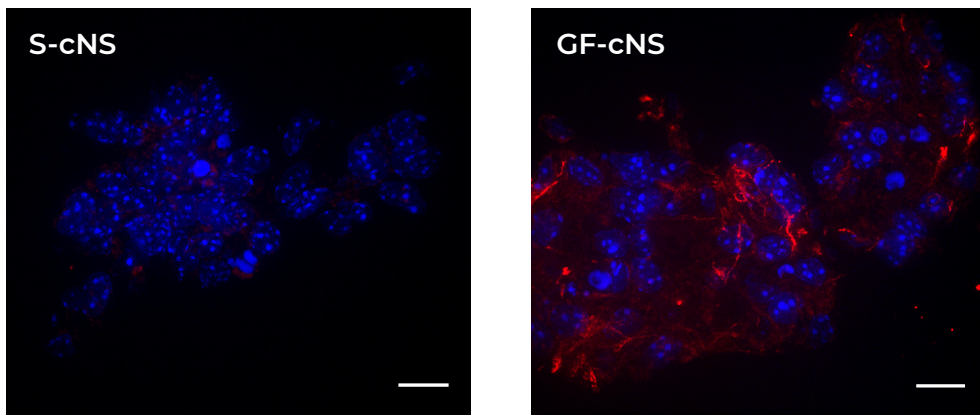


Figure B. Immunofluorescence analysis of Nestin protein. S-cNS and GF-cNS neurospheres stained for Nestin (red) and DNA (blue). GF-cNS neurospheres, unlike S-cNS, show high expression of Nestin. Scale bar, 10 μ m.

To further address whether S-cNS accounted for GCPs, both these and GF-cNS were induced to differentiate. S-cNS derived cells displayed the typical neuron-like morphology characterized by a fusiform cell body extending few neurites of different lengths. Moreover, the vast majority of them expressed the neuronal marker β 3-tubulin, GABRA6 and VGLUT1 proteins (**Figure C**),

suggesting their differentiation into GCs. By contrast, a vast majority of GF-cNS-derived cells acquired a star-shaped GFAP-positive phenotype and only occasionally showed a β 3-tubulin-positive neuron-like appearance (**Figures C and D**), thereby suggesting a glial determination. Moreover, GF-cNS cellular population was completely negative for GABRA6 and VGLUT1 proteins (**Figure C**).

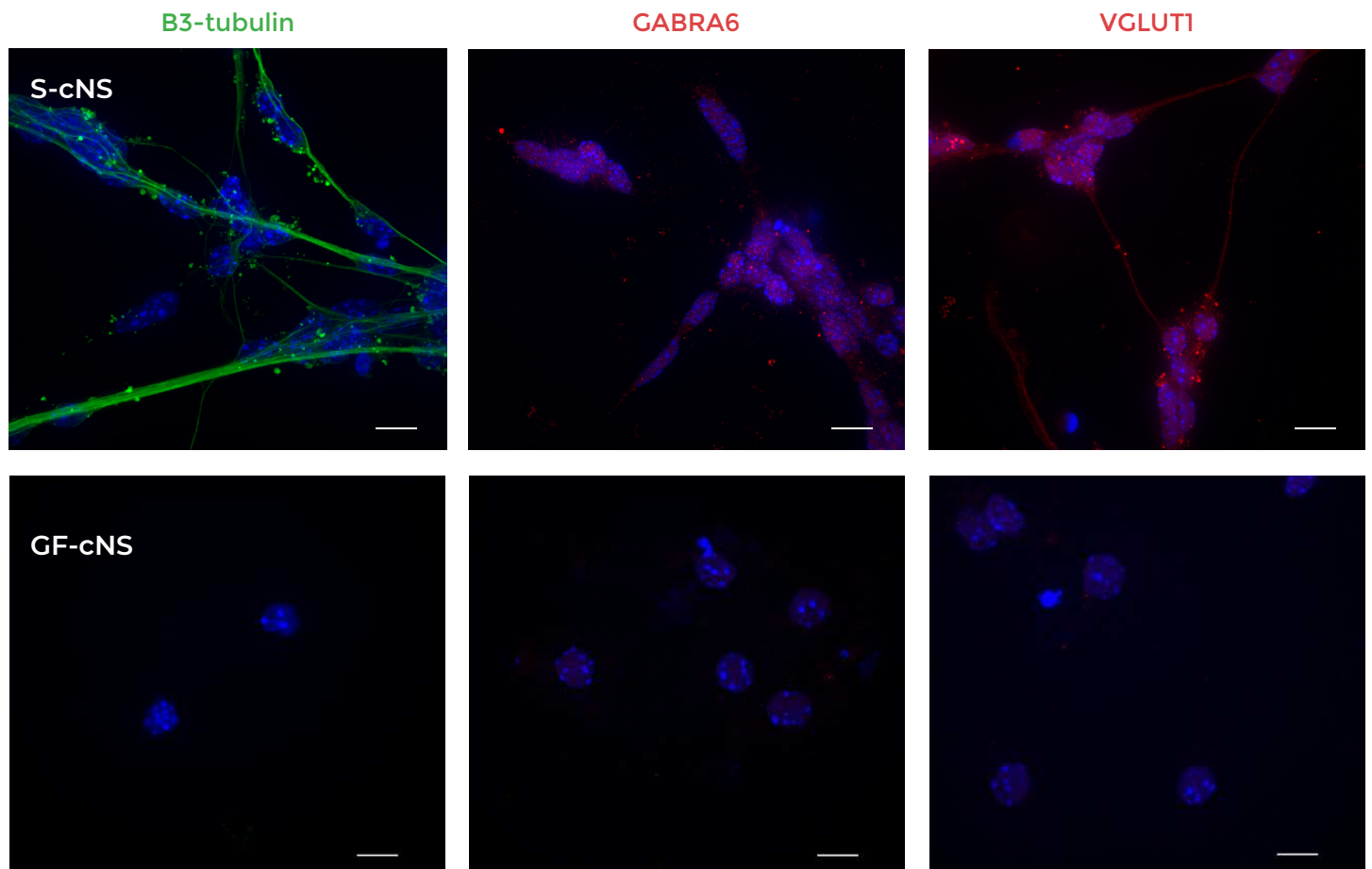


Figure C. Immunofluorescence analysis of B3-tubulin, GABRA6 and VGLUT1 proteins. S-cNS and GF-cNS neurospheres stained for B3-tubulin (green), GABRA6 (red), VGLUT1 (red) and DNA (blue). S-cNS neurospheres, unlike GF-cNS, show high expression of neuronal markers. Scale bar, 10 μ m.

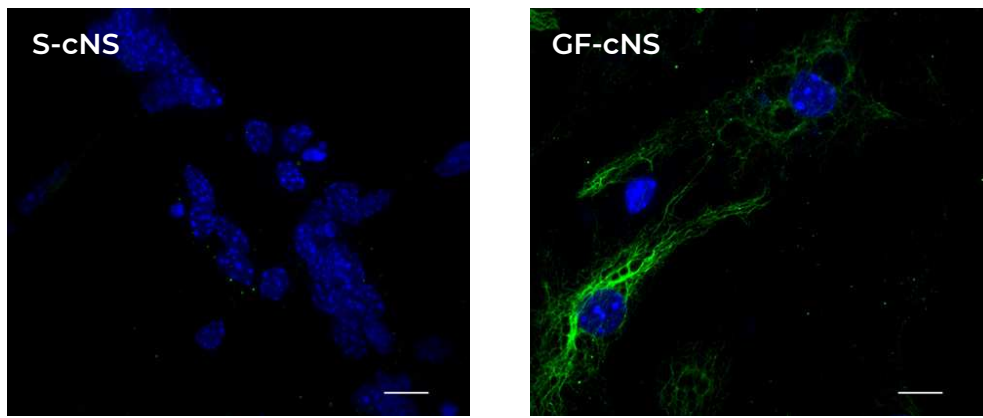


Figure D. Immunofluorescence analysis of GFAP protein.
S-cNS and GF-cNS neurospheres stained for GFAP (green) and DNA (blue). GF-cNS neurospheres, unlike S-cNS, show high levels of GFAP glial marker. Scale bar, 10 μ m.

These data thereby indicate that S-cNS represent a novel long-term and nearly homogenous population of proliferating, non-transformed GCPs *in vitro* that are maintained in culture through the activation of the SHh pathway (via SAG).

SHh drives the expansion of Atoh-1 positive GCPs to coordinate appropriate cerebellar histogenesis. The complex regulation of this pathway has been partially elucidated. In the absence of SHh, the 12-pass transmembrane receptor Patched 1 (Ptch1) constitutively inhibits the seven-pass transmembrane G protein coupled receptor Smoothed (SMO), keeping the pathway inactive. Upon binding of SHh to Ptch1, the inhibition on SMO is alleviated, allowing in turn to the pathway activation. Coherently PTCH1 knock out and some SMO mutations

(e.g. SMO-M2) are both able to induce SHH dependent Medulloblastoma in mice.

Taking advantage of the S-cNS model, the authors uncovered that the PTCH1 knock out, but not the SMO-M2 mutant, is sufficient to maintain a constitutively active SHh pathway and to support GCP survival/proliferation in a cell-autonomous context. The paper suggests that in a SMO-M2 mutant background, PTCH1 may exert at least a partial inhibition on the SMO receptor which may, however, be released by SAG administration. Therefore, the authors demonstrate that S-cNS can be used to address issues related to SHh signaling and, in principle, any other biological and biochemical issue concerning GCPs/GCs in a native and cell-autonomous context.

Methods

S-cNS and GF-cNS cells were fixed with fresh 4% formalin in 0.1 M of phosphate buffer, pH 7.2, for 24 hours at 4 °C. After washing in PBS, neurospheres were centrifuged at 1200 rpm for three minutes at room temperature and frozen in optimal cutting temperature compound. The cryosections were analyzed by immunofluorescence assay for Nestin and Doublecortin (DCX) as indicated in the figure legends. Alternatively, both cultures were seeded on poly-lysine plates and induced to differentiate under opportune condition. Adherent cells were fixed in 3,7% formaldehyde/PBS for 15 minutes at RT and analyzed by immunofluorescence for β 3-tubulin, GABRA6, VGLUT1 and GFAP as indicated in the figure legends. HOECHST

was used to stain cell nuclei (shown in blue). ProLong Glass Antifade Mounting was used (Invitrogen).

The acquisition of the images shown here was performed through a Nikon Eclipse Ti equipped with **X-Light V2 spinning disk (CrestOptics)**, LDI laser source (89 North) and Prime BSI Scientific CMOS (sCMOS) camera with 6.5 μ m pixels (Photometrics). The images were acquired by using Metamorph software version 7.10.2. (Molecular Devices) with a 100x PlanApo Lambda oil objective (1.45 numerical aperture) and sectioning the slice in Z with a step size of 0.1 μ m. Images were elaborated using ImageJ and NIS-Elements AR 5.20 software (Nikon).

Reference

SMO-M2 mutation does not support cell-autonomous Hedgehog activity in cerebellar granule cell precursors ([LINK](#))

Petroni M, Sahùn Roncero M, Ramponi V, Fabretti F, Nicolis Di Robilant V, Moretti M, Alfano V, Corsi A, De Panfilis S, Giubettini M, Di Giulio S, Capalbo C, Belardinilli F, Coppa A, Sardina F, Colicchia V, Pedretti F, Infante P, Cardinali B, Tessitore A, Canettieri G, De Smaele E, Giannini G.

Sci Rep, 2019 Dec 23;9(1):19623. doi: 10.1038/s41598-019-56057-y.